J. Fluid Mech. (1973), *vol.* 59, *part* 4, *pp.* 673–691
Printed in Great Britain

Pressure fields over hypersonic wing-bodies at moderate incidence

By N. MALMUTH
Science Center, Rockwell International, Thousand Oaks, California

(Received 2 October 1972)

Delta wings with conically subsonic cones-bodies mounted on their compressive side are analysed in the hypersonic small disturbance regime. The weakly three-dimensional conditions associated with slender parabolic Mach cones are used to validate a linearized rotational approximation of the flow field. A combined integral–series representation is obtained for the pressure distribution between the wing-body and shock wave for arbitrary body cross-sections, and is specialized to give analytical formulae for arbitrary-order polynomial transversal contours. Numerical results are presented for wedge, parabolic and higher order cross-sections illustrating the dominant character of the cross-flow stagnation singularity associated with sharp wing-body intersections having a finite slope discontinuity. It is shown that the pressure has a logarithmic infinity at this secondary leading edge, as in corresponding Prandtl–Glauert irrotational flows. The relation of this finding to Lighthill's theorem on cross-stream vorticity is discussed. Other features of the pressure field are considered with particular emphasis on their relationship to a recently derived area rule for such configurations, and possibilities for favourable interference.

1. Introduction

An important aspect in the evolution of the new hypersonic vehicles is the effect of wing-body interference on surface pressures and aerodynamic efficiency (L/D). Our understanding of these nonlinear interactions is quite limited, particularly for three-dimensional flows. These facts have motivated extensive application of recent advances in computer technology towards the development of appropriate numerical algorithms. Babaev (1963), Voskresenskii (1968) and South & Klunker (1969) have treated hypersonic conical flows by steepest-descent techniques and the method of lines. Difference methods for hyperbolic systems in three dimensions have recently been employed to handle non-conical geometries (see, for example, Kutler, Lomax & Warming 1972). There have also been investigations such as those by Gunness, Knight & D'Sylva (1972) using simplified numerical formulations based on the hypersonic small disturbance theory (HSDT) of Van Dyke (1954). The utility of these approaches will depend in part on overcoming numerical stability problems near sharp leading edges and shock waves, as well as the attainment of short run times. In certain applications, extensive man–machine interaction is required to handle such instabilities.

Parallel analytic development has shed light on basic physical mechanisms, parametric dependencies and similitudes, and offers the possibility of conditioning the numerical approaches. The simplifications afforded by the HSDT approximation have thus far not been significant enough to lead to many three-dimensional flow solutions of general utility. Newtonian and thin shock-layer theory, which has been shown by Cole (1957) and Hayes & Probstein (1966) to be a subset of HSDT, has been explored for this purpose. Messiter (1963), Cole & Brainerd (1962), Woods (1970), Gonor, Lapygin & Ostapenko (1970), Squire (1968) and Antonov & Hayes (1966), as well as subsequent investigators, have provided valuable insight into compressive flows occurring at the high incidence–Mach number combinations associated with Newtonian or thin-shock-layer approximations.

Cruise applications frequently dictate lower incidence angles for which the thin-shock-layer assumptions are not valid. In this regime, the flow field may be considered weakly three-dimensional for a wide class of practically interesting cases. This realization provides the basis of a systematic approximation scheme embodied in a linearized version of HSDT (LHSDT) which has been used by Malmuth (1966), Ter-Minassiants (1966) and Hui (1971) to treat planar delta wings of moderate aspect ratio. Hayes' unsteady analogy implies a close similarity of these three-dimensional pressure fields to those encountered in weak diffraction of strong shocks, which has been investigated by Lighthill (1950) and his successors. There is some evidence that geometries can be treated by this theory that are of a higher degree of three-dimensionality than would at first seem reasonable from its inherent assumptions.

A recent application of LHSDT has led to the development of an area rule for delta wing bodies given by Malmuth (1971) and extended to lower Mach numbers by Hui (1972). This rule states that the reduction in L/D due to the addition of a conically subsonic cone of arbitrary cross-section on the windward side of a delta wing depends only on the body's cross-sectional area and not its shape. Detailed pressure distributions were not required to prove the rule, since it could be established from integral theorems derived from the boundary-value problem for the perturbation pressure.

In the analysis of Malmuth (1971), a competition between favourable shock diffraction and body pressure drag was suggested to be the controlling mechanism for the body-induced decrement η in the wing-alone inviscid L/D. It was discovered that, for fixed specific heat ratio γ, the quantity η is a monotonic decreasing function of the hypersonic similarity parameter H, where, referring to figure 1(*a*), $H = 1/M_\infty^2\delta^2$, M_∞ = free-stream Mach number and δ = angle of attack, and that there is a critical value of H for which addition of volume actually gives negative values of η. Thus, a kind of favourable interference occurs which differs somewhat from that encountered by Chernyi (1961) and Cole & Aroesty (1965) in connexion with two-dimensional hypersonic airfoils of the type shown in figure 1(*b*). It was shown by these workers that there are classes of profiles that produce reflexions with the shock wave such that suction forces on forwardly inclined surfaces occur, resulting in an interference thrust as shown in figure 1(*b*). In the conical three-dimensional problem, there is no such reflexion process

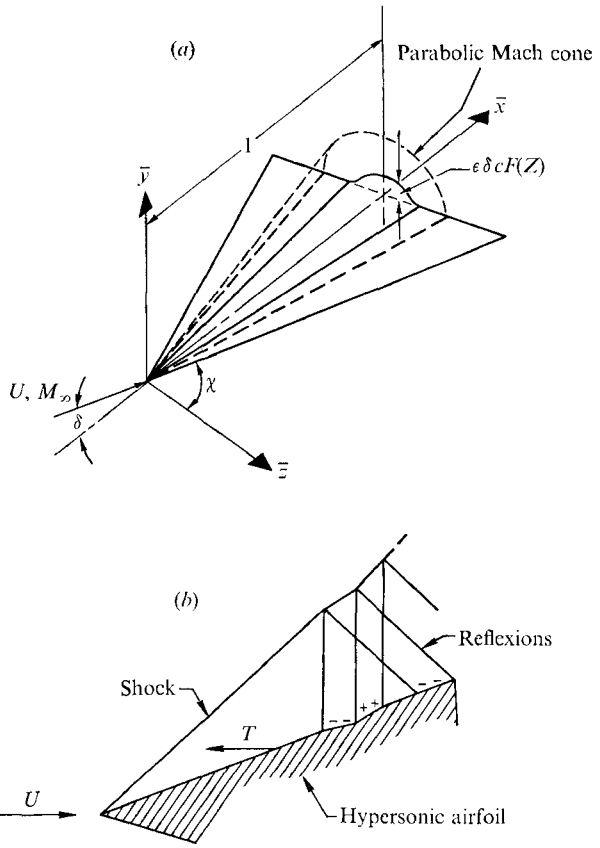

FIGURE 1. (*a*) Wing-body geometry showing free-stream velocity U, Mach number M_∞ (Cartesian axes $\bar{x}$, $\bar{y}$, $\bar{z}$), sweepback angle of leading edge χ and body thickness function F. (*b*) Two-dimensional hypersonic airfoil section with suction on favourably inclined surfaces. $-$, suction zone; $+$, compression zone; T = net interference thrust.

inside the parabolic Mach cone shown in figure 1 (*a*). The benefits at small values of H are due to the changing body portion of the net pressure field of the wing-body combination. Although some insight into this mechanism can be obtained from the relevant integral theorems, a thorough understanding requires the evaluation of the details of the pressure distribution. This information is also necessary for other aerodynamic and structural reasons such as boundary-layer, heat-transfer and flutter calculations.

In this paper, analytic solutions are provided for the pressures over a wide class of delta wing-bodies in hypersonic flow. The boundary-value problem analysed here is a generalization of that treated in Malmuth (1966), which is associated with a planar delta wing at infinite Mach number. In that analysis, an eigenfunction expansion was derived for the pressure field between the wing and shock wave. The eigenfunction coefficients were given by a homogeneous linear first-order difference equation. It will be seen that the analogous difference equations for wing-bodies at finite Mach number are of second order and inhomogeneous. A major thrust of this paper is the derivation of properties of the pressure field

from the solution of these difference equations. In contrast to Malmuth (1966) explicit solutions are obtained for infinite Mach number. For finite values of this parameter, a Green's matrix is derived from which the influence of general conical volume distributions can be readily calculated.

From these results, various features are identified which influence the division of the pressure field between the wing and body. An example of such a property is the behaviour of sharp wing-body intersections as compared with rounded junctions. Numerical results are presented for special shapes illustrating these effects as well as the influence of Mach number and specific heat ratio.

2. Formulation

In the following discussion, the delta wing-body configuration shown in figure 1 (*a*) is treated. The equation of the wing-body is

$$Y-(\epsilon/c)\,F(Z)=0, \quad Y\equiv \bar{y}/c\,\delta\bar{x}, \quad Z\equiv \bar{z}/c\,\delta\bar{x}, \quad \epsilon\equiv\delta\tan\chi,$$

where c is a normalized sound speed, to be defined subsequently. The body thickness function F is assumed to have bounded but not necessarily continuous first derivatives with respect to Z on the interval $0\leqslant Z\leqslant 1$. In addition, F is assumed to be zero outside this range. For the LHSDT limit,

$$H \text{ fixed}, \quad \delta,\epsilon\to 0,$$

the asymptotic expansion for the pressure $\bar{P}$ is

$$[(\bar{P}(x,y,z;M_\infty,\delta,\chi,\gamma)-\bar{P}_\infty]/\delta^2\rho_\infty U^2=p_0[1+\epsilon p(Z,Y;H,\gamma)]+O(\delta^2),$$

where ρ_∞ and U are the free-stream density and velocity respectively, and

$$p_0=\theta+1=\tfrac{1}{4}(\gamma+1)+\{[\tfrac{1}{4}(\gamma+1)]^2+H\}^{\frac{1}{2}}.$$

If $Y=\tanh\sigma$, $Z=\operatorname{sech}\sigma\sin\mu$ and $Y_s\equiv\theta/c$, $c\equiv\theta[\theta+\frac{1}{2}(\gamma+1)]$, the boundary-value problem for the perturbation pressure p in the σ, μ plane is

$$\left[\frac{\partial^2}{\partial\sigma^2}+\frac{\partial^2}{\partial\mu^2}\right]p=0 \quad \text{in the region } R\colon 0\leqslant\sigma\leqslant\sigma_s=\tanh^{-1}Y_s,\ 0\leqslant\mu\leqslant\tfrac{1}{2}\pi, \tag{1a}$$

$$\partial p(0,\sigma)/\partial\mu=p(\tfrac{1}{2}\pi,0)=0, \tag{1b}$$

$$\left[\frac{\partial}{\partial\sigma}+(\bar{c}_1\sin^2\mu+\bar{c}_2)\operatorname{cosec}\mu\sec\mu\frac{\partial}{\partial\mu}\right]p=0 \quad \text{on} \quad \sigma=\sigma_s, \tag{1c}$$

$$\bar{c}_1\equiv-2\bar{c}_2[1-(\gamma+1)/4(\theta+1)], \quad \bar{c}_2\equiv\tfrac{1}{2}(\coth\sigma_s),$$

$$\partial p(\mu,0)/\partial\sigma=\phi(\mu)\equiv-Y_s^{-1}\sin^2\mu F''(Z), \tag{1d}$$

$$\int_0^{Z_M}Z^{-1}\frac{dp}{dZ}\,dZ=\frac{4c\theta}{\gamma+1} \text{ on } Y=Y_s, \quad Z_M\equiv[1-Y_s^2]^{\frac{1}{2}}. \tag{1e}$$

The region R corresponds to the portion of the flow bounded by the parabolic Mach cone, wing-body and shock wave.

3. Solution

With quantities associated with the planar delta wing ($F=0$) denoted by superscript zero, the perturbation pressure can be decomposed into two components:

$$p=p^{(0)}+\Delta p,$$

where Δp is the body-induced increment in pressure. It can be shown that this represents a decomposition of $(1a\text{–}e)$ into a problem for $p^{(0)}$, corresponding to a flat-plate delta wing, and another for Δp, associated with a body on an upswept wing. The geometric features of the wing and body in the component problems are identical to those in the composite wing-body problem for p.

By a generalization of the analysis of Malmuth (1966), the solution of $(1a\text{–}e)$ is

$$p^{(0)} = \sum_0^\infty A_n^{(0)} \frac{\cos(2n+1)\mu \cosh(2n+1)\sigma}{2n+1}, \tag{2a}$$

$$\Delta p = \sum_0^\infty \frac{\cos(2n+1)\mu}{2n+1} [\Delta A_n \cosh(2n+1)\sigma + B_n \sinh(2n+1)\sigma], \tag{2b}$$

$$\Delta A_n \equiv A_n - A_n^{(0)}, \quad B_n = \frac{4}{\pi}\int_0^{\frac{1}{2}\pi} \phi(\mu)\cos(2n+1)\mu\, d\mu. \tag{2c,d}$$

To facilitate the determination of ΔA_n, an infinite Green's matrix $\mathbf{k}$ can be defined such that

$$\Delta A_n = \sum_{m=0}^\infty k_{nm} B_m. \tag{2e}$$

Equations $(1c)$ and $(1e)$ are used to obtain the following recursion relations for the $A_n^{(0)}$ and k_{nm}:

$$\left.\begin{aligned} &M_n[A_n^{(0)}] = 0, \quad n \geqslant 0, && (3a)\\ &b_0' A_1^{(0)} + c_0' A_0^{(0)} = 0, && (3b)\\ &\sum_0^\infty A_n^{(0)} c_{2n+1} = -8c\theta/\pi(\gamma+1)c_1, && (3c) \end{aligned}\right\}$$

$$\left.\begin{aligned} &M_n[k_{nm}] = N_n[\delta_{nm}], \; n \geqslant 0, && (3d)\\ &b_0' k_{1m} + c_0' k_{0m} = f_0' \delta_{1m} + g_0' \delta_{0m}, && (3e)\\ &\sum_{n=0}^\infty c_{2n+1} k_{nm} = -s_{2m+1}, && (3f) \end{aligned}\right\}$$

where δ_{nm} is the Kronecker delta and

$$c_n \equiv \cosh n\sigma_s, \quad s_n \equiv \sinh n\sigma_s,$$

$$M_n \equiv a_n E^2 + b_n E + c_n^*, \quad N_n \equiv d_n E^2 + f_n E + g_n, \quad E y_n \equiv y_{n+1},$$

$$4a_n \equiv s_{2n+5} - \bar{c}_1 c_{2n+5}, \quad b_n \equiv (\bar{c}_2 + \tfrac{1}{2}\bar{c}_1) c_{2n+3}, \quad -4c_n^* \equiv s_{2n+1} + \bar{c}_1 c_{2n+1},$$

$$-4d_n \equiv c_{2n+5} - \bar{c}_1 s_{2n+5}, \quad -f_n \equiv (\bar{c}_2 + \tfrac{1}{2}\bar{c}_1) s_{2n+3}, \quad 4g_n \equiv c_{2n+1} + \bar{c}_1 s_{2n+1},$$

$$4b_0' \equiv s_3 - \bar{c}_1 c_3, \quad c_0' \equiv (\bar{c}_2 + \tfrac{3}{4}\bar{c}_1) c_1 - \tfrac{1}{4} s_1, \quad 4f_0' \equiv c_3 - \bar{c}_1 s_3, \quad g_0' \equiv (\bar{c}_2 + \tfrac{3}{4}\bar{c}_1) s_1 - \tfrac{1}{4} c_1.$$

The difference equations $(3a\text{–}f)$ may be more easily solved if the 'conservation' conditions $(3c)$ and $(3f)$ are replaced by initial conditions. This can be achieved by use of integral theorems developed in Malmuth (1971). Defining the relevant spanwise pressure integrals as,

$$P(Y) \equiv \int_0^{[1-Y^2]^{\frac{1}{2}}} p\, dZ = \int_0^{\frac{1}{2}\pi} p \operatorname{sech}\sigma \cos\mu\, d\mu,$$

$$P^{(0)} \equiv \int_0^{[1-Y^2]^{\frac{1}{2}}} p^{(0)}\, dZ,$$

the integral theorems are

$$P^{(0)} = 2c^2/(\gamma+1)\,\alpha, \tag{4a}$$

$$\Delta P \equiv P - P^{(0)} = [1-(\alpha^{-1}+Y)/Y_s]\,V, \tag{4b}$$

where

$$\alpha \equiv -\tfrac{1}{2}c[8/(\gamma+1)+(2\theta-\gamma+3)/2\theta(\theta+1)],$$

$$V \equiv 2\int_0^1 F\,dZ = \text{body volume}.$$

Integration of $(2a)$ and $(2b)$ and comparison with $(4a)$ and $(4b)$ gives

$$A_0^{(0)} = 8c^2/\pi(\gamma+1)\,\alpha, \quad k_{0m} = (\alpha^{-1}-Y_s)\,\delta_{0m}. \tag{3c',f'}$$

At $M_\infty = \infty$, explicit solutions for $A_n^{(0)}$ and k_{nm} are facilitated since M_n and N_n have a common factor, and the order of the equations may thereby be reduced. In particular,

$$4M_n = (E+1)\,[E\alpha_n - \beta_n], \quad 4N_n = (E+1)\,[E\gamma_n + \delta_n],$$

$$\alpha_n \equiv s_{2n+1} + \bar{c}_2 c_{2n+1}, \quad \beta_n \equiv s_{2n+1} - \bar{c}_2 c_{2n+1},$$

$$-\gamma_n \equiv c_{2n+1} + \bar{c}_2 s_{2n+1}, \quad \delta_n \equiv c_{2n+1} - \bar{c}_2 s_{2n+1},$$

so that

$$(E+\mu_n)\,A_n^{(0)} = 0, \tag{5a}$$

$$(E+\mu_n)\,k_{nm} = (\bar{\omega}_{n+1}E + \omega_n)\,\delta_{nm}, \tag{5b}$$

where

$$\mu_n \equiv (\bar{c}_2 c_{2n+1} - s_{2n+1})/(\bar{c}_2 c_{2n+3} + s_{2n+3}),$$

$$-\bar{\omega}_n \equiv (c_{2n+1} + s_{2n+1})/(s_{2n+1} + \bar{c}_2 c_{2n+1}),$$

$$\omega_n \equiv (c_{2n+1} - \bar{c}_2 s_{2n+1})/(\bar{c}_2 c_{2n+3} + s_{2n+3}).$$

Noting that $(5a)$ includes $(3b)$, and $(5b)$ includes $(3e)$, the variation of parameters method for linear difference equations yields the following solutions:

$$A_n^{(0)}/A_0^{(0)} \equiv R_n \equiv \prod_0^{n-1}(-\mu_k), \quad R_0 \equiv 1, \tag{6a}$$

$$k_{nm}/R_n = k_{0m} + (\omega_m H_{n-m-1} H_m - \mu_m \bar{\omega}_m H_{n-m} H_{m-1})/R_{m+1}, \tag{6b}$$

where

$$H_k = \begin{cases} 0, & k < 0, \\ 1, & k \geqslant 0, \end{cases}$$

and the second term in $(6b)$ vanishes for $n = 0$.

It should be noted that the k_{nm} are independent of the body shape and depend only on H and γ. Accordingly, they can be calculated once and for all, and used with $(2e)$ to evaluate the 'induced' pressure of volume on the delta wing. From $(6b)$, it is demonstrated that $\mathbf{k}$ is a triangular matrix, with its row elements a rapidly decreasing sequence downward. This property holds for arbitrary H, and gives a rapidly converging sum for the ΔA_n in $(2e)$.

4. Cross-flow stagnation singularities

To isolate singular elements, $(2b)$ is rewritten using Kummer's transformation as

$$\Delta p = \sum_0^\infty [(\Delta A_n + B_n)\cosh(2n+1)\,\sigma\cos(2n+1)\,\mu]/(2n+1) - S(\mu,\sigma), \tag{2b'}$$

where

$$S \equiv \sum_0^\infty B_n e^{-(2n+1)\,\sigma}[\cos(2n+1)\,\mu]/(2n+1). \tag{7}$$

From (2*e*) and (3*d*), $k_{mn}+\delta_{nm}$ and ΔA_n+B_n are $O(e^{-\alpha n})$ as $n\to\infty$, where $\alpha > 2\sigma_s$. Thus, the first series in (2*b*′) will be rapidly convergent even for $B_n = O(1)$ as $n\to\infty$. This case occurs if F' has a finite jump discontinuity on $0 \leqslant Z \leqslant 1$, and gives logarithmically slow convergence for $S(0,\mu)$. To avoid this difficulty, an integral representation for (7) is used. This can be easily obtained on substitution of (2*d*) and interchanging summation and integration, which is justifiable by uniformity of convergence for $\sigma \neq 0$. The evaluation of $\lim_{\sigma\to 0} S(\sigma,\mu)$ thereby corresponds to an Euler summation. From well-known summation identities,

$$S = \int_0^{\frac{1}{2}\pi} \phi(\mu')\, G_S(\sigma,\mu;\mu')\, d\mu', \tag{8a}$$

where

$$G_S(\sigma,\mu;\mu') \equiv \frac{1}{2\pi}\ln\left(\frac{1-2e^{-\sigma}\cos(\mu+\mu')+e^{-2\sigma}}{1+2e^{-\sigma}\cos(\mu+\mu')+e^{-2\sigma}}\right)\left(\frac{1-2e^{-\sigma}\cos(\mu-\mu')+e^{-2\sigma}}{1+2e^{-\sigma}\cos(\mu-\mu')+e^{-2\sigma}}\right). \tag{8b}$$

Specializing, the surface distribution of body-induced incremental pressure is thus

$$\Delta p(\mu,0) = \frac{1}{\pi}\int_0^{\frac{1}{2}\pi} \phi(\mu')\,[\tanh^{-1}\cos(\mu+\mu')+\tanh^{-1}\cos(\mu-\mu')]\,d\mu' + \sum_0^\infty (\Delta A_n+B_n)\,[\cos(2n+1)\mu]/(2n+1). \tag{9}$$

To fix the ideas, consider a class of F functions such that $F(Z) = \psi(Z)H(Z_0-Z)$, where $\psi(Z_0) = 0$, $Z_0 \equiv \sin\mu_0$, H is the Heaviside function and $\psi(Z)$ is regular on $0 \leqslant Z \leqslant Z_0 < 1$. It is of interest to establish the singular nature of the pressure field near the resulting sharp wing-body ridge line at Z_0. From (1*d*),

$$\phi(\mu) = -Y_s^{-1}[Z_0^2\sec\mu_0\,\delta(\mu_0-\mu)\,\psi'(Z_{0-}) - Z^2\psi''(Z)\,H(\mu_0-\mu)], \tag{10}$$

where $\delta(x)$ is the Dirac delta function and $\psi'(Z_{0-}) \equiv \lim_{\epsilon\to 0}\psi'(Z_0-\epsilon)$. To treat the first term on the left-hand side of (10), define the surface Green's function as

$$\Delta p = \int_0^{\frac{1}{2}\pi} G(\mu,\sigma;\mu')\,\phi(\mu')\,d\mu'. \tag{11}$$

From (2*b*′), (2*d*) and (8*a*) it follows that

$$G(\mu,\sigma;\mu') = -G_S(\sigma,\mu;\mu') + \frac{4}{\pi}\sum_{n=0}^{\infty}\left[\cos(2n+1)\mu' + \sum_{m=0}^{\infty} k_{nm}\cos(2m+1)\mu'\right] \times [\cosh(2n+1)\sigma\cos(2n+1)\mu]/(2n+1). \tag{12a}$$

If $\psi''(Z) = 0$ (the case of a transverse wedge), (10) and (11) yield

$$\Delta p_{\text{wedge}} = -Z_0^2\sec\mu_0\,G(\mu,\sigma;\mu_0)/Y_s. \tag{12b}$$

It is evident from the rapid convergence of the second term in (12*a*) that the singular behaviour of Δp near the point $(0,\mu_0)$ is due to G_S, which can be written in terms of the complex variable $z \equiv \mu + i\sigma$ as

$$G_S(\sigma,\mu;\mu_0) = \frac{1}{\pi}\ln|\tan\tfrac{1}{2}(z-\mu_0)\tan\tfrac{1}{2}(z+\mu_0)| \doteq \frac{1}{\pi}\ln|z-\mu_0| \quad \text{as} \quad z\to\mu_0. \tag{13a}$$

In LHSDT, the vorticity is the same order as the pressure perturbations. However, (13*a*) shows a qualitative resemblance to the behaviour of geometrically similar irrotational Prandtl–Glauert flows at lower Mach numbers, studied extensively by Jones & Cohen (1957). Lighthill (1949) has shown that the pressure field is unaffected by cross-stream vorticity in this regime. However, it remains to be shown that the case under consideration fulfills the conditions of his theorem.

The second factor in the argument of the logarithm of (13*a*) represents an image effect of the 'source' singularity comprising the first, and is required to satisfy the second condition in (1*b*). Accordingly, if $\mu_0 = \frac{1}{2}\pi$, the singular behaviour of the pressure becomes that of a 'doublet' at $z = \frac{1}{2}\pi$:

$$-\pi G_S \doteq (z-\tfrac{1}{2}\pi)^{-1} \quad \text{as} \quad z \to \tfrac{1}{2}\pi. \tag{13b}$$

For the case of an arbitrary polynomial cross-section

$$\psi = \sum_0^N \alpha_n Z^n \tag{14a}$$

with the previous restrictions

$$B_n = B_n^{(S)} + B_n^{(R)}, \tag{14b}$$

where

$$B_n^{(S)} \equiv \left(4\left[\cos(2n+1)\mu_0\right] \sum_{m=1}^{N} \alpha_m m Z_0^{m+1}\right) \Big/ \pi(1-Z_0^2)^{\frac{1}{2}} Y_s, \tag{14c}$$

$$B_n^{(R)} = -\left(4 \sum_{m=2}^{N} m(m-1)\, I_{nm}\right) \Big/ \pi Y_s, \tag{14d}$$

$$I_{nm}(\mu_0) \equiv \int_0^{\mu_0} \sin^m \mu \cos(2n+1)\mu \, d\mu. \tag{14e}$$

Of the many possible representations for the integral (14*e*) the following are the most advantageous for computation:

$$I_{n0}(\mu) = \frac{\sin(2n+1)\mu}{2n+1}, \tag{14f}$$

$$I_{n,2p} = 4^{-p}\left\{\sum_{k=0}^{p-1}(-1)^{p-k}\binom{2p}{k}\{(\sin[2(p+n-k)+1)\mu]/[2(p+n-k)+1] + [\sin(2(p-n-k)-1)\mu]/[2(p-n-k)-1]\} + \binom{2p}{p}(\sin(2n+1)\mu)/(2n+1)\right\}, \quad p > 0, \tag{14g}$$

$$I_{01} = \tfrac{1}{4}(1-\cos 2\mu), \tag{14h}$$

$$I_{n,2p-1} = -2(4^{-p})\left\{\sum_{k=0}^{p-1}{}' (-1)^{p+k-1}\binom{2p-1}{k}[\{(\cos 2(p-k+n)\mu)-1]/2(p-k+n) + [\cos(2(p-k-n-1)\mu)-1]/2(p-k-n-1)\}\right\} \quad (n > 0), \tag{14i}$$

where $\binom{a}{b} \equiv (a!)/(a-b)!\,b!$, the binomial coefficient, $p = 1, 2, 3 \ldots$, and the prime on the sum in (14*i*) signifies that the last two terms are to be omitted whenever the denominator vanishes, i.e. $p = k+n+1$.

−0·8819	0	0	0	0	0...
0·3713	−9·9747	0	0	0	0
−0·03861	0·08021	−0·9948	0	0	0
0·002748	−0·005708	0·01654	−0·9989	0	0
−0·0001771	0·0003680	−0·001067	0·003380	−0·9998	0
$1{\cdot}1179 \times 10^{-5}$	$-2{\cdot}322 \times 10^{-5}$	$6{\cdot}729 \times 10^{-5}$	−0·0002133	0·0006891	−1
⋮					

TABLE 1. Structure of matrix **k**; $H = 0$, $\gamma = 1{\cdot}4$

−0·9871	0	0	0	0...
0·05465	−0·9993	0	0	0
0·01781	0.002944	−1	0	0
−0·002299	0·0009632	0·0001576	−1	0
$2{\cdot}540 \times 10^{-4}$	$-1{\cdot}224 \times 10^{-4}$	$5{\cdot}158 \times 10^{-5}$	$8{\cdot}435 \times 10^{-6}$	−1
⋮				

TABLE 2. Structure of matrix **k**; $H = 1$, $\gamma = 1{\cdot}4$

−0·9943	0	0.	0...
0·002915	−1	0	0
0·0001335	$2{\cdot}281 \times 10^{-5}$	−1	0
$-2{\cdot}216 \times 10^{-5}$	$1{\cdot}044 \times 10^{-5}$	$1{\cdot}784 \times 10^{-7}$	−1
⋮			

TABLE 3. Structure of matrix **k**; $H = 10$, $\gamma = 1{\cdot}4$.

5. Results and discussion

Tables 1, 2 and 3 show the structure of the matrix **k** for $H = 0$, 1 and 10, and $\gamma = 1{\cdot}4$. Consistent with previous observations, the effect of the higher body cross-sectional area moments on the volume-induced interference pressure Δp appears to be small. An increasing volume effect on span loading can be shown for increasing bow shock strength, since k_{00}/Y_s increases with decreasing H. How the actual induced pressures Δp compare with the wing-alone component $p^{(0)}$ will now be discussed in connexion with specific cross-sectional shapes.

The singular behaviour associated with a sharp, conically subsonic, wing-body juncture is most clearly evaluated from the wedge cross-section. A typical example selected for illustration of the effect is

$$F = (\tfrac{1}{2} - Z)\, H(\tfrac{1}{2} - Z)\, H(Z), \tag{15}$$

for which (12*b*) gives Δp directly. Figure 2(*a*) shows the surface pressure distribution associated with (15) (on $Y = \sigma = 0$) for $H = 1$ and $\gamma = 1{\cdot}4$. As in the infinite Mach number case, studied in Malmuth (1966), the wing-alone perturbation pressure $p^{(0)}$ demonstrates a monotonic decay towards the centre-line, $Z = 0$. This smooth expansion is a general feature of the flow field for all H and is associated with turning of the streamlines away from the line of symmetry resulting from the bow shock's compression of the component of the free stream normal to the wing leading edge. The streamline pattern associated with this conically invariant expansion process can be easily visualized, since the perturbation in the free-stream direction is negligible to the order of the approximations,

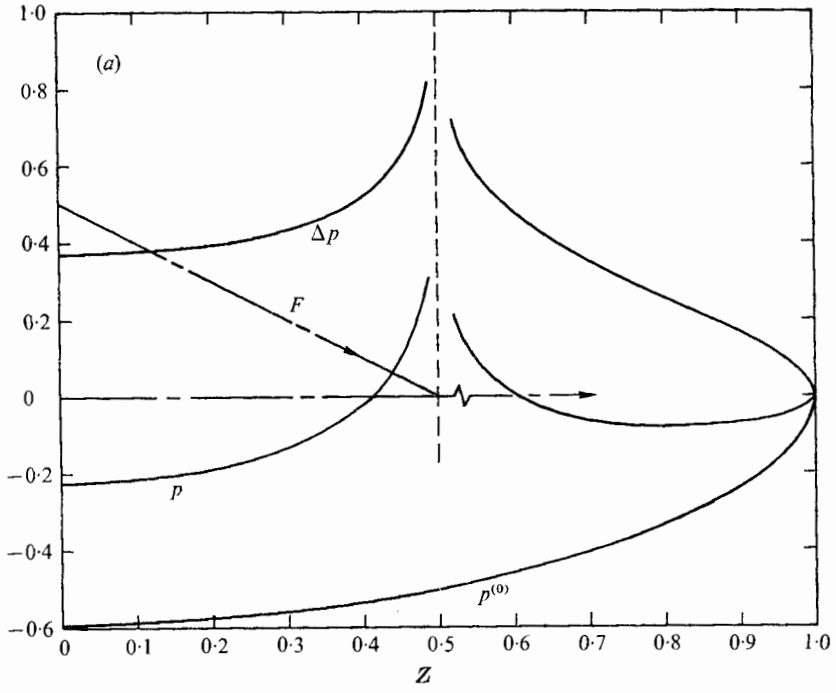

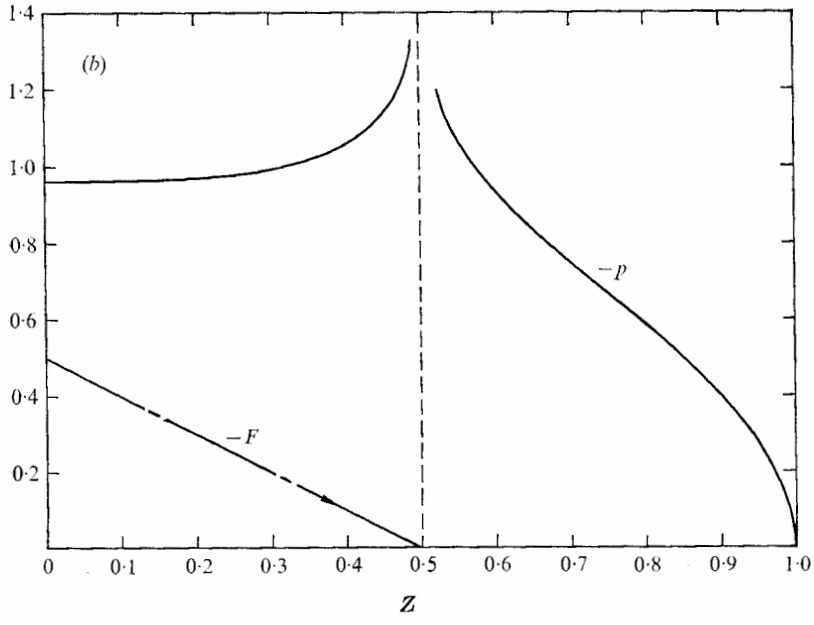

FIGURES 2(*a*, *b*). For legend see page 683.

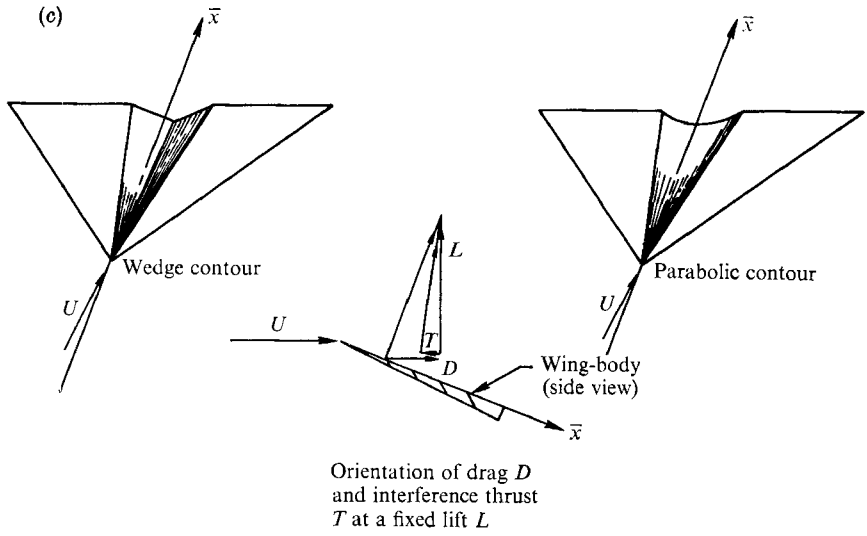

FIGURE 2 (*a*). Surface spanwise pressure distributions. $p^{(0)}$ = basic delta-wing perturbation pressure, Δp = body-induced increment of perturbation pressure, p = resultant perturbation pressure = $p^{(0)}+\Delta p$, ψ = body thickness function, Z = physical spanwise conical co-ordinate, $H = 1, \gamma = 1{\cdot}4, \psi = \frac{1}{2}-Z$. (*b*) Surface spanwise pressure distributions. $H = 1$, $\gamma = 1{\cdot}4, \psi = -\frac{1}{2}+Z$. (*c*) Wedge and parabolic concave delta wing bodies.

and the sidewash varies smoothly from its positive value at the shock to zero, required by symmetry, at the centre-line. The behaviour of the volume-induced effect Δp demonstrates that the compressive nature of the singularity at $Z = Z_0 = \frac{1}{2}$ is felt immediately downstream of the Mach cone $\mu = \frac{1}{2}\pi$ owing to the subsonic nature of the cross-flow cone field. Because the secondary compression near Z_0 is qualitatively similar to that just discussed in connexion with the leading edge, a similar recovery phenomenon is exhibited, in which Δp decays from the logarithmic singularity given by (13*b*) near Z_0 to a finite positive value at $Z = 0$. It should be noted that the ridge-line slope discontinuity at this location associated with the last factor on the left-hand side of (15) has no effect, since its centre-line orientation prevents its modification of the sidewash field. This is confirmed by the presence of the $\sin^2\mu$ factor in (1*d*).

For the associated 'concave' body in which the sign of F in (15) is reversed, the only change in p is a corresponding sign change for Δp. The corresponding net pressure is shown in figure 2 (*b*). It is obvious that there is an interesting trade off here between lost volume and attendant interference thrust, for various H and γ. For purposes of visualization of the implied geometries, sketches of wedge and parabolic concave wing bodies are shown in figure 2 (*c*).

In figure 3, the behaviour of the pressure field over the wing-edge body is shown. The rapid attenuation of the leading-edge singularity is quite evident from these distributions.

The effect of increased shock strength at lower H is typified in figure 4. It is evident that the body contribution represents a much larger fraction of the net pressure field than at lower Mach number and incidence. This is consistent with

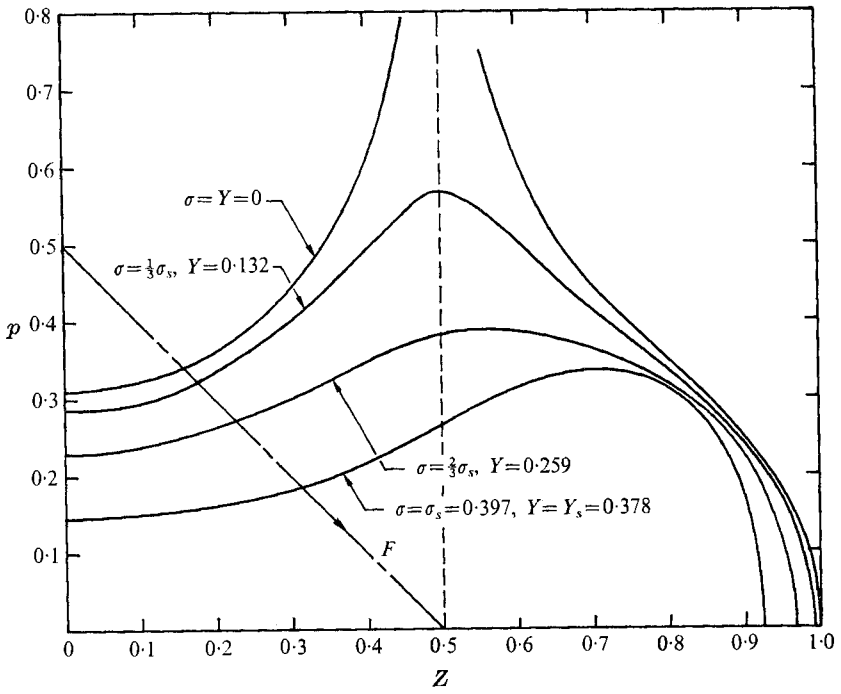

FIGURE 3. Vertical variation of pressure distributions. σ = transformed vertical conical co-ordinate, Y = physical vertical conical co-ordinate. $H = 0, \gamma = 1{\cdot}4, \psi = \frac{1}{2} - Z$.

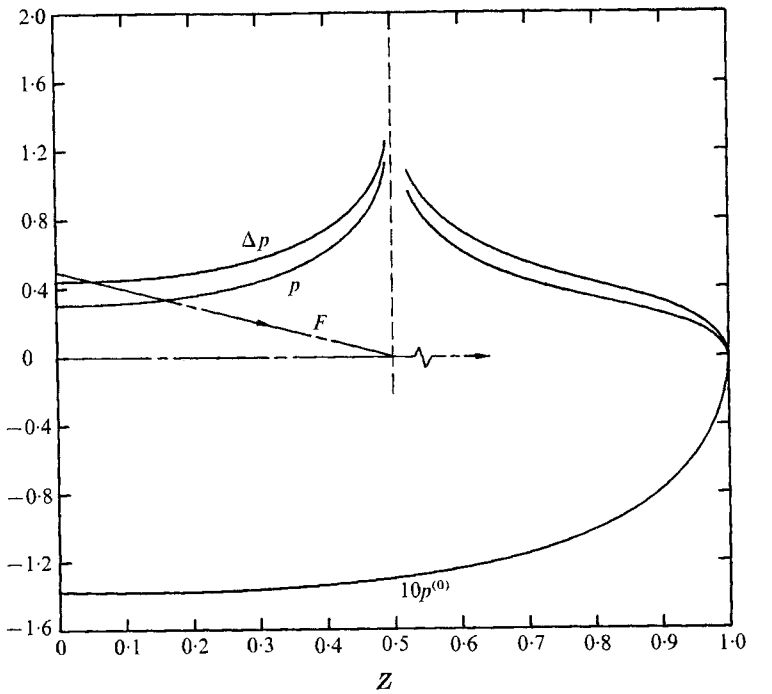

FIGURE 4. Surface spanwise pressure distributions. $H = 0, \gamma = 1{\cdot}4, \psi = \frac{1}{2} - Z$.

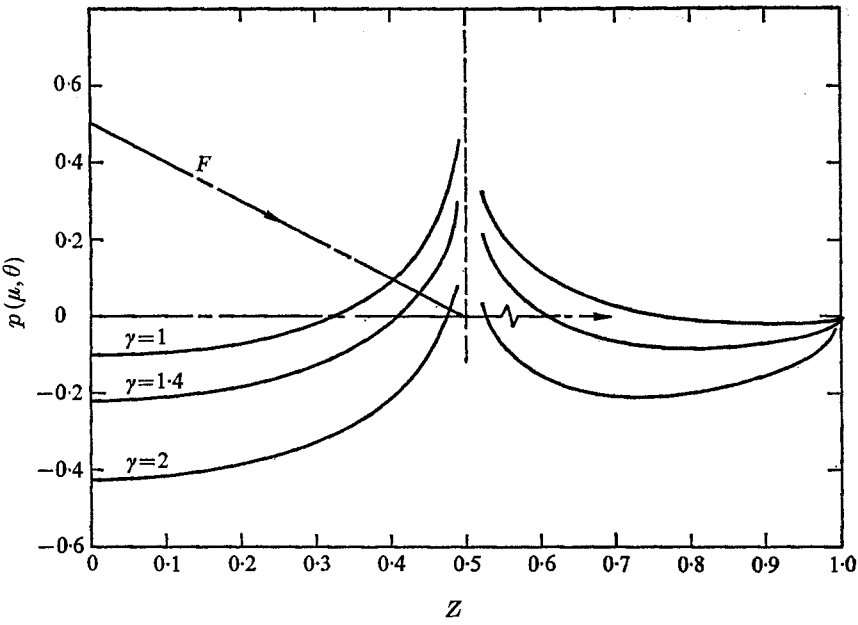

FIGURE 5. Effect of γ on surface pressures.

a 'figure of merit' study by Malmuth (1971) in which a benefit in wing-alone L/D could be achieved with volume addition for sufficiently low values of H. Figure 5 shows the effect of the specific heat ratio γ on this apportionment.

Pressure distributions for higher order profiles such as those with $N = 2$ and 3 in (14a) are indicated in figures 6–8 for the cases in which ψ has no zeros on $0 \leqslant Z \leqslant Z_0$. The quantity Δp exhibits the same qualitative features as those associated with zero transverse curvature, $N = 1$.† These characteristics are dominated by the stagnation singularity at Z_0, the superposed wing-alone expansion field, the centre-line recovery from cross-flow stagnation conditions. rapid attenuation of the singularity with elevation and increasing $\Delta p/p_0$ with $H \to 0$.

In contrast to the case $N = 1$, for $N > 1$, $B_n(R) \neq 0$. For the cases considered. acceptable convergence in (2b') required 50 terms in the summation. Procedures for acceleration of convergence were not implemented owing to the facility of the computational algorithm. Typical cases were accessible by digital equipment within seconds.

Since sharp ridge lines are structurally untenable, it is of interest to establish modifications in the loading associated with 'blended' wing-bodies with F' continuous at Z_0. For this purpose, the quadratic ($N = 2$) and cubic ($N = 3$) profiles shown in figure 9 lead to the indicated pressure distributions. As for $N = 1$, no singularity occurs owing to the kink at $Z = 0$ for the quadratic, or any other polynomial with $F'(0) \neq 0$. This fact is justified in the same manner as

† The behaviour of $\partial p/\partial Z$ at the 'triple point' ($\frac{1}{2}\pi$, σ_s) is discussed in the appendix.

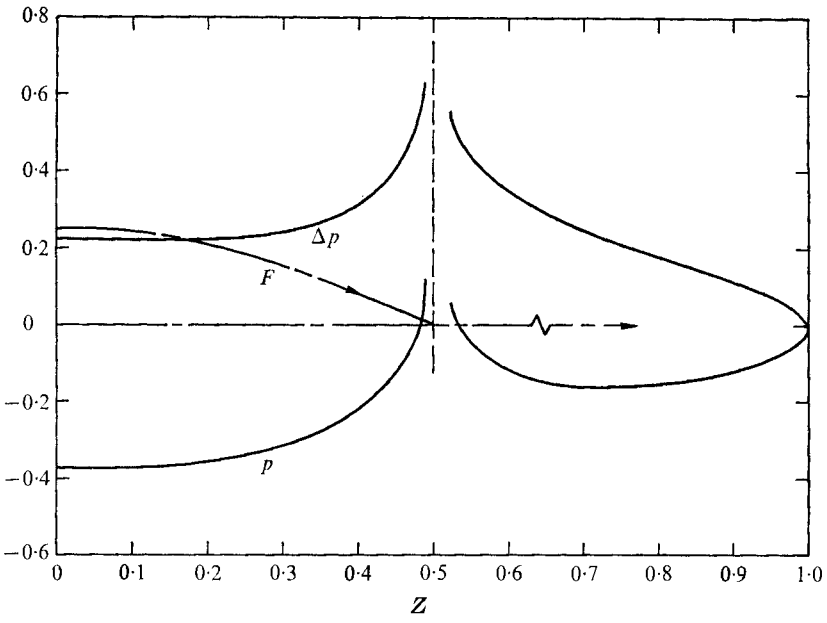

FIGURE 6. Surface spanwise pressure distributions. $H = 1$, $\gamma = 1{\cdot}4$, $\psi = \frac{1}{4} - Z^2$.

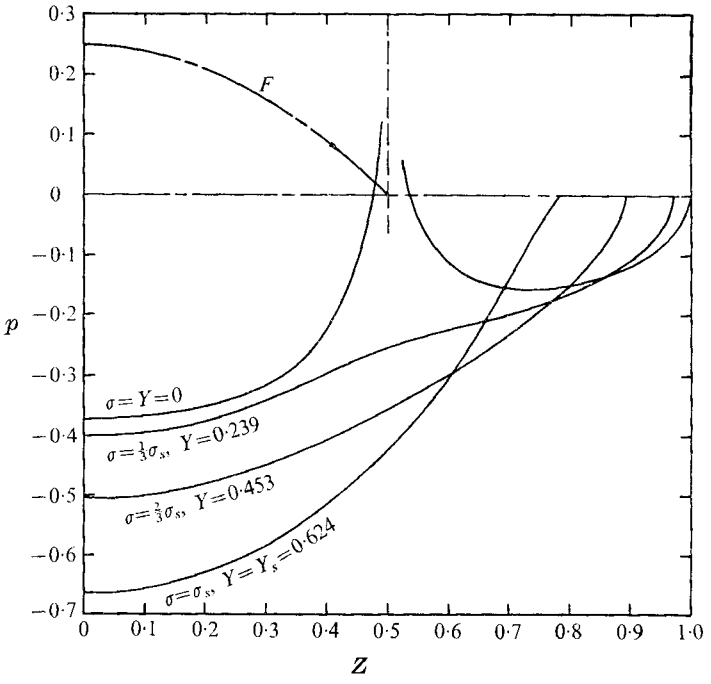

FIGURE 7. Vertical variation of pressure distributions. $H = 1$, $\gamma = 1{\cdot}4$, $\psi = \frac{1}{4} - Z^2$.

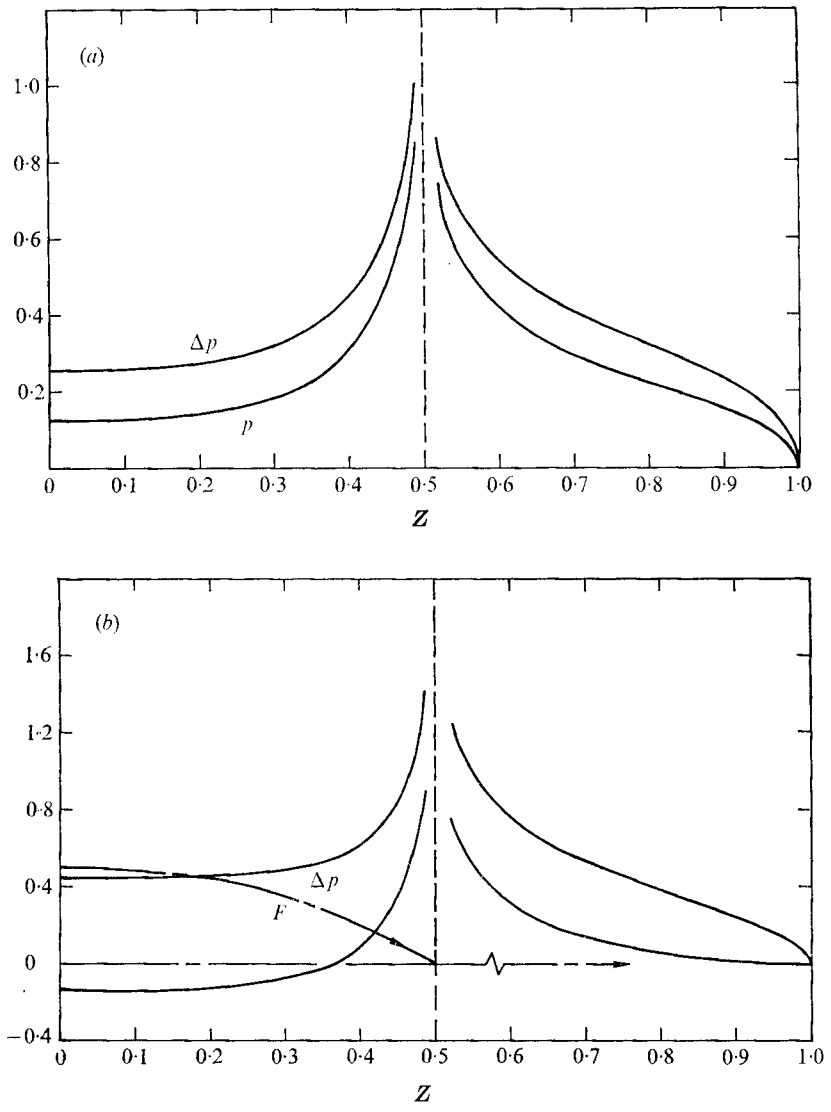

FIGURE 8. Surface spanwise pressure distributions. $\gamma = 1{\cdot}4$. (*a*) $H = 0$, $\psi = \frac{1}{4} - Z^2$. (*b*) $H = 1$, $\psi = \frac{1}{2} - Z^2 - 2Z^3$.

before. It is evident that the logarithmic singularity has been removed by the blending, but there is considerable compression near the wing-body junction region which is relieved by the previously described expansion process towards the centre-line.

Interesting effects occur for the reflex profile shown in figure 10, for which

$$\psi = \tfrac{1}{16} - Z^2 + Z^3 + Z^4.$$

In this case, ψ has a zero on $0 \leqslant Z \leqslant Z_0$ and the previous observation regarding the dominant effect of the leading-edge singularity no longer holds. This is evident from the compression occurring in the region $Z_0 \leqslant Z \leqslant 1$ which is due to

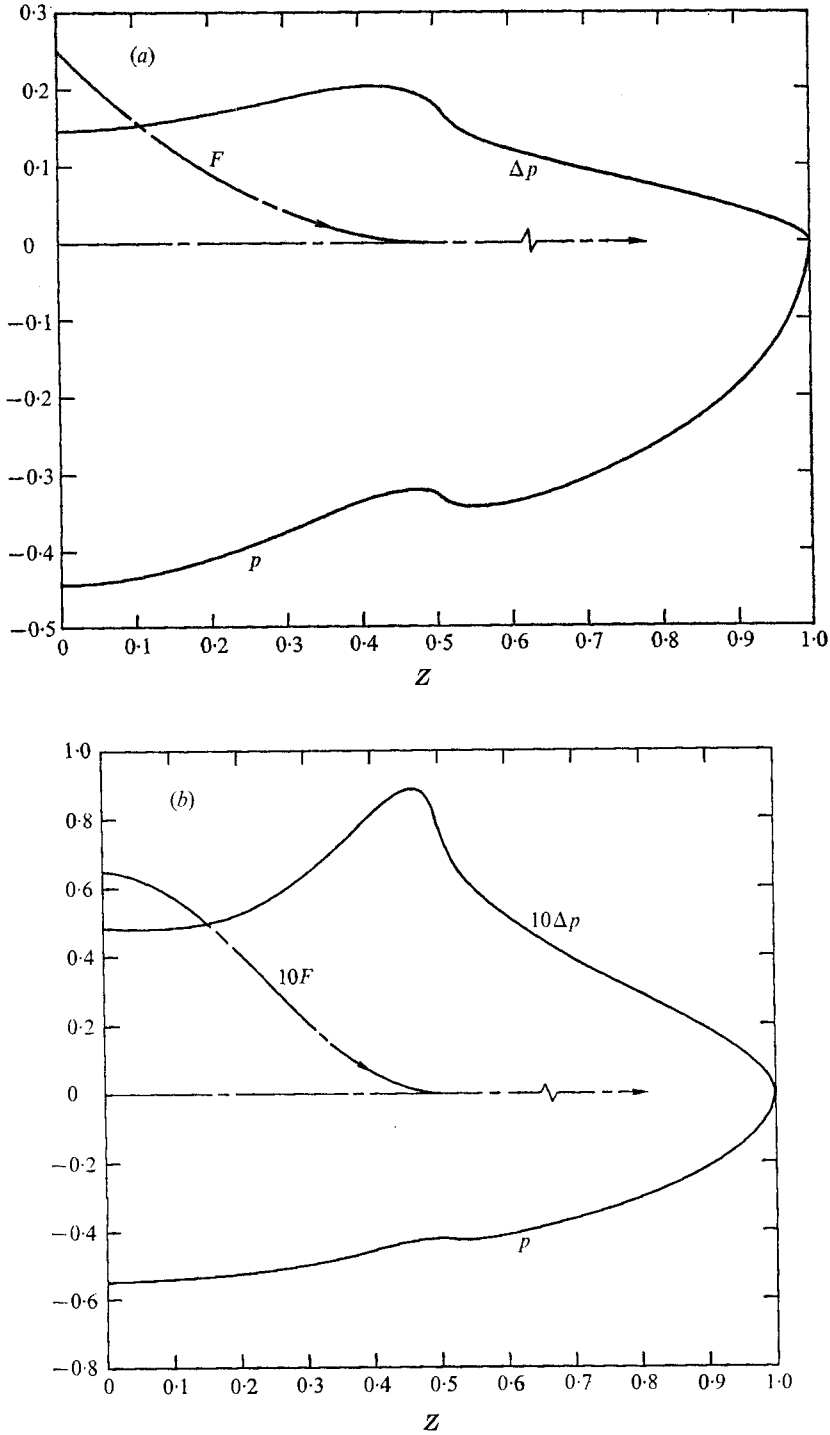

FIGURE 9. Surface spanwise pressure distributions. $\gamma = 1{\cdot}4$, $H = 1$. (*a*) $\psi = \frac{1}{4} - Z - Z^2$. (*b*) $\psi = \frac{1}{16} - \frac{3}{4}Z^2 + Z^3$.

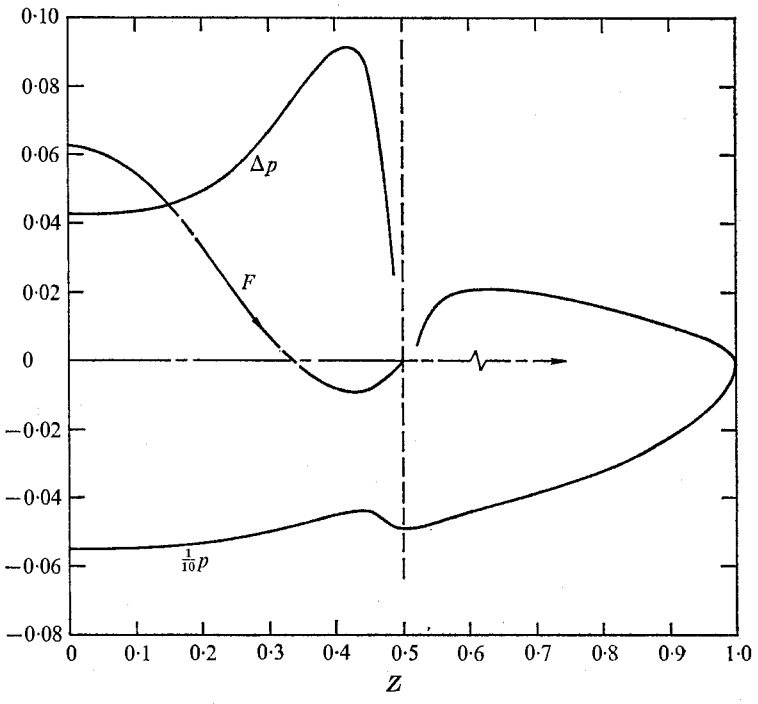

FIGURE 10. Surface spanwise pressure distributions.
$H = 1$, $\gamma = 1{\cdot}4$, $\psi = \frac{1}{16} - Z^2 + Z^3 + Z^4$.

the overwhelming effect of the central part of the body. The influence of this section far outweighs the logarithmic singularity everywhere, except in its immediate neighbourhood.

6. Summary and conclusions

It has been shown that a general class of conical wing-body interactions may be treated using an analogue of the rotational linearized theory of weakly diffracted strong shocks. A combined integral–series representation has been obtained for the pressure field over a slender, conically subsonic cone of arbitrary cross-section on the compressive side of a delta wing, for the weakly three-dimensional hypersonic small disturbance limit discussed in Malmuth (1966). A logarithmic stagnation singularity associated with a finite slope discontinuity at the wing-body junction is exhibited by the pressure formula. General features of the pressure field are as follows.

(i) The body component of the net pressure of the combination increases relative to the wing-alone portion for increasing Mach number and incidence.

(ii) If the volume distribution is one signed, the pressure field is dominated by the secondary leading-edge singularity if the juncture is sharp. This behaviour is qualitatively similar to that predicted by irrotational Prandtl–Glauert theory at lower Mach numbers, suggesting the relevance of Lighthill's theorem on the independence of irrotational pressure fields to imposed cross-stream vorticity.

(iii) The influence of the stagnation singularity attenuates rapidly with elevation above the wing.

(iv) Concave wing-bodies may produce significant interference thrust.

(v) Concave bodies give an equal and opposite contribution to net wing-body pressure as compared with convex ones of the same shape.

(vi) 'Blended' wing-body combinations round off the logarithmic singularity occurring with sharp junctures. There is still considerable overshoot in the pressure, with a substantial decay near the centre-line owing to symmetry and the superposed expansion field of the wing.

It is conjectured that many of these conclusions will apply qualitatively to thicker delta-wing mounted bodies in the HSDT regime.

This study was supported by the Air Force Office of Scientific Research (AFSC) United States Air Force, under Contract F 44620-71-C-0021. The author acknowledges valuable comments by J. D. Cole in the early phases of the research.

Appendix

The singular nature of the 'triple point' intersection of the conically subsonic and supersonic limbs of the shock $Y = Y_s$ with the Mach cone $\mu = \frac{1}{2}\pi$ has been the subject of some previous investigations. Various workers have treated 'corner boundary layers' within the framework of thin shock layer and second-order irrotational linearized theories. In this paper, the pressure variations shown in the figures suggest similar singularities. In particular, it appears that $(\partial f/\partial Z) \to -\infty$ as $\mu \uparrow \frac{1}{2}\pi$ for $0 \leqslant \sigma \leqslant \sigma_s$ if $H = 0$, where $f = p^{(0)}$, Δp or p. Moreover if $H \neq 0$, the same behaviour holds, except at the triple point $(\frac{1}{2}\pi, \sigma_s)$, where $\partial f/\partial Z$ is bounded (cf. figure 7). These facts will now be corroborated from the properties of a harmonic Taylor expansion about the triple point which is written as

$$f = \sum_{n=0}^{\infty} \sum_{m=0}^{\infty} a_{nm} \xi^n \eta^m, \tag{A 1}$$

where $\xi = \mu - \frac{1}{2}\pi, \quad \eta = \sigma - \sigma_s.$

From (1*a–c*) it can be shown that, for $H \neq 0$,

$$\begin{aligned} -f/a_{11} &= \xi\eta + (\xi^3 - 3\xi\eta^2)/(\bar{c}_1 + \bar{c}_2) + \ldots \\ &\doteq [2(1 - Z/Z_M)]^{\frac{1}{2}} (Y - Y_s)/Z_M^2 + \ldots \quad (Z_M \equiv \operatorname{sech} \sigma_s), \end{aligned}$$

so that

$$\begin{aligned} \partial f/\partial Z &\sim (1 - Z/Z_M)^{-\frac{1}{2}} \quad \text{as} \quad Z \to Z_M, \quad Y \text{ fixed}, \quad 0 \leqslant Y < Y_S, \\ 0 &< \partial f/\partial Z < \infty \quad \text{as} \quad Z \to Z_M, \quad Y = Y_S. \end{aligned} \tag{A 2}$$

Thus, the triple point is a saddle singularity for the isobars in the σ, μ plane.

For $H = 0$, the triple point changes in character, since (1*c*) reduces to

$$\left(\frac{\partial}{\partial \sigma} + (2Y_s)^{-1} \cot \mu \frac{\partial}{\partial \mu}\right) f = 0 \quad \text{on} \quad \sigma = \sigma_s.$$

Accordingly $$f \sim (1 - Z/Z_M)^{\frac{1}{2}}$$

and $\partial f/\partial Z$ behaves as in (A 2) on the closed interval $0 \leqslant Y \leqslant Y_S$, verifying the hypothesis.

REFERENCES

ANTONOV, A. M. & HAYES, W. D. 1966 Calculation of the hypersonic flow about blunt bodies. *J. Appl. Math. Mech.* **30**, 421–427.

BABAEV, D. A. 1963 Numerical solution of the problem of flow around the lower surface of a delta wing. *A.I.A.A. J.* **1**, 2224–2231.

CHERNYI, G. G. 1961 *Introduction to Hypersonic Flow* (trans. & ed. R. F. Probstein), pp. 181–191. Academic.

COLE, J. D. 1957 Newtonian flow theory for slender bodies. *J. Aero Sci.* **24**, 448–455.

COLE, J. D. & AROESTY, J. 1965 Optimum hypersonic lifting surfaces close to flat plates. *A.I.A.A. J.* **3**, 1520–1522.

COLE, J. D. & BRAINERD, J. J. 1962 Slender wings at high angles of attack. In *Hypersonic Flow Research* (ed. F. R. Riddell), pp. 321–343. Academic.

GONOR, A. L., LAPYGIN, N. I. & OSTAPENKO, N. A. 1970 The conical wing in hypersonic flow. In *Proc. 2nd Int. Conf. on Numerical Methods in Fluid Dyn., Lecture Notes in Physics*, vol. 8, pp. 320–334.

GUNNESS, R. C., KNIGHT, C. J. & D'SYLVA, E. 1972 Flow field analysis of aircraft configurations using a numerical solution to the three-dimensional unified supersonic/hypersonic small disturbance equations. Part I. *N.A.S.A. Contractor Rep.* CR-1926.

HAYES, W. D. & PROBSTEIN, R. F. 1966 *Hypersonic Flow Theory*. vol. I. *Inviscid Flows*. Academic.

HUI, W. 1971 Supersonic and hypersonic flow with attached shock waves over delta wings. *Proc. Roy. Soc.* A **325**, 251–268.

HUI, W. H. 1972 Unified area rule for hypersonic and supersonic wing bodies. *A.I.A.A. J.* **10**, 961–962.

JONES, R. T. & COHEN, D. 1957 Aerodynamics of wings at high speeds. In *Aerodynamic Components of Aircraft at High Speeds*, vol. 7, pp. 14–21.

KUTLER, P., LOMAX, H. & WARMING, R. F. 1972 Computation of space shuttle flow fields using non-centred finite difference schemes. *A.I.A.A. Paper*, no. 72–193.

LIGHTHILL, M. J. 1949 The flow behind a stationary shock. *Phil. Mag.* **40**, 214–220.

LIGHTHILL, M. J. 1950 The diffraction of blast. II. *Proc. Roy. Soc.* A **200**, 554–565.

MALMUTH, N. D. 1966 Hypersonic flow over a delta wing of moderate aspect ratio. *A.I.A.A. J.* **4**, 555–556.

MALMUTH, N. D. 1971 A new area rule for hypersonic wing-bodies. *A.I.A.A. J.* **9**, 2460–2462.

MESSITER, A. F. 1963 Lift of slender delta wings according to Newtonian theory. *A.I.A.A. J.* **1**, 794–802.

SOUTH, J. C. & KLUNKER, E. B. 1969 Methods for calculating nonlinear conical flows. In *Analytical Methods in Aircraft Aerodynamics Symposium – published Proceedings held at Moffett Field Calif., N.A.S.A. Rep.* SP-228, pp. 131–158.

SQUIRE, L. C. 1968 Calculated pressure distributions on conical wings with attached shock waves. *Aeron. Quart.* **19**, 31–50.

TER-MINASSIANTS, S. M. 1966 Supersonic flow around the lower surface of a delta wing. *Izv. Akad. Nauk SSSR, Mekhzhidk Gaza*, **6**, 147–152.

VAN DYKE, M. D. 1954 A study in hypersonic small disturbance theory. *N.A.C.A. Tech. Note*, no. 3173.

VOSKRESENSKII, G. P. 1968 Numerical solution of the problem of a supersonic gas flow past an arbitrary surface of a delta wing in the compression region. *Izv. Akad. Nauk SSSR Mekhzhidk Gaza*, **4**, 134–142.

WOODS, B. A. 1970 Hypersonic flow with attached shock waves over delta wings. *Aeron. Quart.* **21**, 379–399.